Conference paper

Setare Tahmasebi Nick, Ali Bolandi, Tova A. Samuels and Sherine O. Obare*

Advances in understanding the transformation of engineered nanoparticles in the environment

Abstract: Engineered nanoparticles (ENPs) are known to possess unique size and shape dependent chemical and physical properties. As a result of their properties, ENPs have been effective in several important applications including catalysis, sensor design, photonics, electronics, medicine, and the environmental remediation of toxic pollutants. Such properties and applications have led to an increase in the manufacture of ENPs and a rise in their presence in consumer products. The increase of ENPs in consumer products presents several opportunities and challenges, and necessitates a proactive study of their health and safety. This article highlights some recent work in which we have studied the effect of exposure of well-defined ENPs to pesticides and the effect of pH and dissolved organic matter. We also summarize our work and that of others who have studied the toxicity of ENPs with microorganisms. The results provide insights on the need for green manufacturing strategies of ENPs, their use and safe disposal practices.

Keywords: dissolved organic carbon (DOC); engineered nanoparticles (ENPs); environmental chemistry; IUPAC Congress-44; microorganisms; organothiophosphorus (OTP) pesticides; surface plasmon resonance (SPR).

DOI 10.1515/pac-2014-0301

Introduction

The design and use of engineered nanoparticles (ENPs) is a rapidly emerging field offering a multitude of technological opportunities, some of which are in use while others are yet to be uncovered [1–13]. The unique chemical and physical properties of ENPs relative to their bulk counterparts have resulted in the use of ENPs in several consumer products. The increased manufacturing and use of ENPs, their unique properties, and high reactivity has raised concerns of their release into the environment during their life cycle. Thus, ENPs are emerging contaminants and there is an increasing interest toward understanding their fate, transport, bioavailability, environmental safety and toxicological effects. Studies have shown the risks of exposure for individuals who work in the manufacture of, or production of consumer products containing ENPs [14–18]. The chemical composition, surface reactivity, solubility, aggregation tendency and increased surface to volume

Article note: A collection of invited papers based on presentations on the Environmental Chemistry theme at the 44th IUPAC Congress, Istanbul, Turkey, 11–16 August 2013.

***Corresponding author: Sherine O. Obare,** Department of Chemistry, Western Michigan University, Kalamazoo, MI 49008, USA, e-mail: sherine.obare@wmich.edu
Setare Tahmasebi Nick, Ali Bolandi and Tova A. Samuels: Department of Chemistry, Western Michigan University, Kalamazoo, MI 49008, USA

ratio of ENPs renders them highly reactive, and how their reactivity influences species in the environment raises several health and toxicological concerns [19–24]. The properties of ENPs rely significantly on the particle composition, size, shape, dispersity, and morphology [25–29]. Furthermore, the method by which ENPs are prepared has a profound effect on their structure and surface. As a result, significant efforts are currently being devoted toward developing '*green*' methods, where the process of nanoparticle design reduces or eliminates use of hazardous chemicals, and the process is carried out in aqueous solvent, to minimize their toxicity [30].

Several manufactured ENPs are currently commercially available, while others are being developed in research laboratories. Studies to understand the health and safety of ENPs are usually conducted using commercially available ENPs mainly because they are most likely to enter the environment relative to those that are not in the market. Concerns have been raised that when studies are conducted to understand the toxicity of ENPs, the uniformity in particle size, shape, and morphology of commercially obtained ENPs are often poor leading to results that are often not reproducible. Lack of ENPs that are homogenous makes understanding the reactivity or behavior of ENPs in the environment difficult since the reactivity of ENPs is highly dependent on size, shape and morphology. Consequently, a major goal in the study of the toxicity of ENPs is to design and have access to well-defined particles. Thus, one of the major goals of our group is to develop straightforward synthetic procedures for the production of well-defined metallic, nanoparticles in high yield [31–34].

Studies that are conducted to understand the transformation of ENPs in the environment must take into account interactions that occur with metal ions, dissolved organic matter, environmental contaminants for example pesticides, and microorganisms. The interaction of ENPs with dissolved organic carbon (DOC) is an important area of investigation. How DOC affect ENPs will govern the effect of these particles on microbial species, the biota and the ecosystem. DOCs can adsorb on the surface of metal nanoparticles, which impact ENP dispersion and affect the particle fate, transport, bioavailability and toxicity. Humic acids (HA) are the main components of DOCs and are therefore representative model systems to use in ENP studies. HA tends to absorb metal ions and hydrous metal oxides due to their structural features [35]. Furthermore, environmental pH plays an important role on the amount of HA absorbed on the ENPs due to changes in the particle surface charge [36]. A number of reports have studied the influence of DOC on the behavior of ENPs both in aqueous environments and with respect to impact on microorganisms [37, 38]. High ionic strength has also been found to result in the aggregation of ENPs due to the repulsion of the charges on the nanoparticle surface [39]. Therefore, ionic strength is an important parameter to study when determining ENP toxicity since aggregation will affect the particle mobility and transport potential and influence the fate and toxicity [40].

In this article, we highlight some of our work involving the interaction of well-defined metallic ENPs with pesticide contaminants. We further describe the work of others involving the interaction of metallic ENPs with microorganisms. We note that much of the work performed in the area of metallic nanoparticles focuses on the use of gold (Au) and silver (Ag) nanoparticles (NPs), and there is a need to further study the effects of other emerging metallic nanoparticles.

Interaction of ENPs with organothiophosphorus pesticides

One class of pollutants that are found in the environment include organothiophosphorous (OTP) pesticides (Fig. 1). These compounds are highly toxic to human health and are powerful inhibitors of cholinesterase enzymes [41, 42]. Unfortunately, frequent use of OTP pesticides in urban areas, agricultural lands, and farm animals, has resulted in their acute presence as residuals in homes, on crops and livestock, and has further led to their migration into surface water and groundwater [43–45]. The emergence of metal NPs in the environment will lead to possible interactions with OTPs and it is important to understand how the NPs interact with OTP pesticides under environmental conditions.

To study the interaction between OTPs and NPs, we prepared colloidal solutions of monodisperse silver nanoparticles (Ag NPs) in ultrapure milli Q water. The Ag NPs were prepared by the chemical reduction of

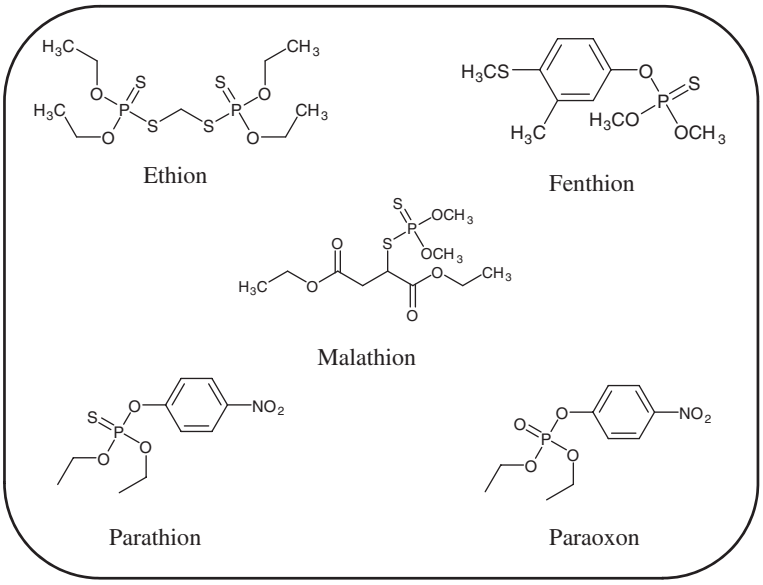

Fig. 1 Chemical structure of common organophosphorus pesticides.

silver nitrate ($AgNO_3$) by sodium borohydride using sodium citrate ($Na_3C_6H_5O_7$) as the stabilizing agent. The solution mole ratio of stabilizing agent: metal species: reducing agent was 1:1:1. The nanoparticle solutions were characterized by UV-visible absorbance spectroscopy and electron microscopy, and stored in the dark until used.

One of the unique features of Ag NPs is that they display a surface plasmon resonance (SPR) band at 390–420 nm depending on their size and dispersity. Changes in the SPR could provide insights of the nanoparticles undergoing agglomeration or dissolution. The Ag NPs we used in this study were 4 nm in diameter and displayed a SPR band at 390 nm. To investigate the interaction of the Ag NPs with OTP pesticides, we titrated a colloidal solution of Ag NPs with parathion, fenthion, malathion, and ethion [all in millimolar (mM) concentrations of pesticide], and compared the results to the titration of a non-OTP pesticide, paraoxon. Figure 1 shows the chemical structure of the OTP pesticides studied. UV-visible absorbance spectroscopy was used to characterize any changes in the Ag NP surface plasmon resonance (SPR) band as the pesticide concentration was increased. SPR measurements were made 10 min after the addition of the pesticide to the Ag NP solution. Titrations were performed in triplicate. Transmission electron microscopy (TEM) was also used to characterize any changes in nanoparticle size and distribution after addition of the pesticide to each Ag NP solution.

The titration of Ag NPs with OTP pesticides caused the initial SPR band at 390 nm to decrease in absorbance intensity, while an additional lower energy SPR absorbance band peak formed. A representative titration of Ag NPs with parathion is shown in Fig. 2. At a final concentration of 1.99×10^{-3} M parathion, the colloidal Ag NPs exhibited two SPR peaks at 390 nm and 556 nm and was accompanied by color change of the Ag NP solution from yellow to deep orange. Similar results were observed with fenthion, ethion and malathion. The peak at 390 nm represents the SPR peak and its decrease in intensity accompanied by broadening indicates that the nanoparticles are losing their homogeneity. Furthermore, the formation of the peak at 556 nm indicates that the particles are undergoing agglomeration with increasing parathion concentration. The yellow colored colloidal Ag NP solutions underwent colorimetric titrations with solutions of parathion, and were characterized at the concentrations shown in Fig. 2 via UV-visible absorbance spectroscopy. Figure 2 shows the changes in SPR absorbance bands and solution color as the concentration of parathion was increased.

The changes in the SPR band of the colloidal Ag NPs is believed to be largely due to the soft acid-soft base interactions between the NPs and the sulfur atom of the thiophosphoryl group (P=S) in the OTPs, according to the hard-soft acid-base theory [46]. Sulfur atoms (soft base) are expected to favorably interact with Ag atoms (soft acid) such that the surface charge of the NPs is disrupted, leading to destabilization of the colloid, and

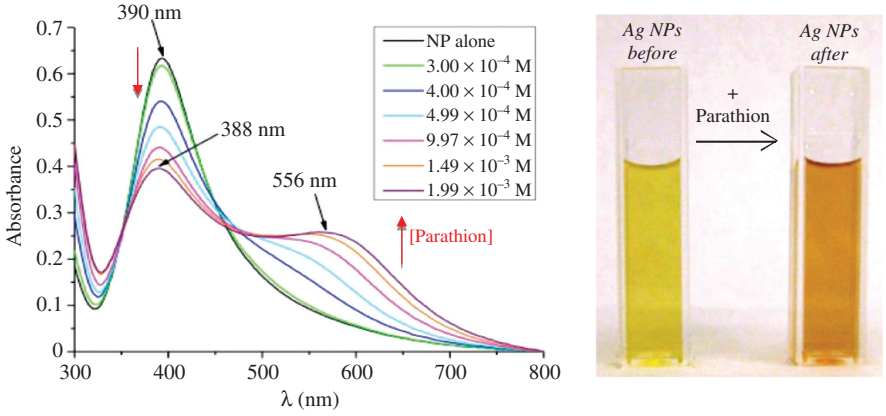

Fig. 2 Changes in the colloid SPR absorbance band and colloid color of Ag NPs upon the interaction with parathion. The red arrows indicate the direction of the SPR peak with increasing parathion concentration.

a change in the collective plasmon resonance. To verify this hypothesis, a control experiment was carried out with the nanoparticles and paraoxon-ethyl, which has a phosphoryl (P = O) constituent rather than a P = S. The oxygen atom is considered a hard base, and therefore is not expected to favorably interact with the Ag atoms. The colloidal nanoparticle solutions were each titrated with 1×10^{-3} M paraoxon-ethyl. Figure 3 shows that the Ag NPs were not affected by paraoxon-ethyl at saturation concentrations (~3.32×10^{-6} M), such that no change in SPR absorbance band or solution color was observed. The TEM images show significant nanoparticle agglomeration for Ag NPs interacting with parathion relative to paraoxon-ethyl as shown in Fig. 4.

The colorimetric response of the colloidal metal NPs was verified under simulated fresh surface water, whereby humic acid was present and the pH was adjusted to 6.5. UV-visible absorbance spectroscopy was used to characterize any optical changes, and TEM imaging was used to characterize any changes to the colloid morphology and interparticle distance. Colloidal solutions of Ag NPs were titrated with parathion in the presence of 6.3 mg C/*l* humic acid (where C represents the mass of dissolved organic carbon per unit volume) and at pH 6.5. The SPR absorbance spectra of Ag NPs responding to increasing concentrations of OTP pesticides obtained under environmental conditions was dramatically different as compared to titrations without simulated environmental conditions. After the addition of 6.3 mg C/*l* humic acid, and pH adjustment to 6.5, the Ag NPs' SPR band maximum red shifted from 392 nm to 397 nm and decreased in absorbance intensity (Fig. 5). Furthermore, the Ag colloids exhibited a light brown color. These optical changes differed from the SPR absorbance band and color changes observed when titrating parathion in the absence of humic acid, which exhibited two SPR peaks and a color change to deep orange.

Ag NP colloids in the presence of humic acid were also titrated with a paraoxon-ethyl solution to a final concentration of 3.32×10^{-6} M, to observe their response to a control analyte. At the final concentration of

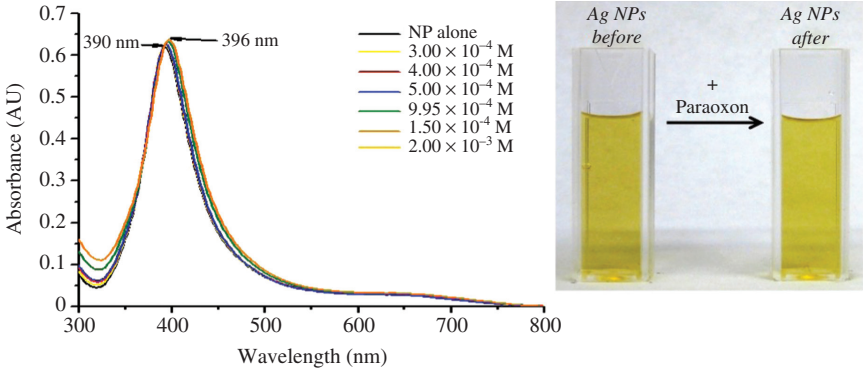

Fig. 3 Changes in the colloid SPR absorbance band and colloid color of Ag NPs upon titration with paraoxon-ethyl.

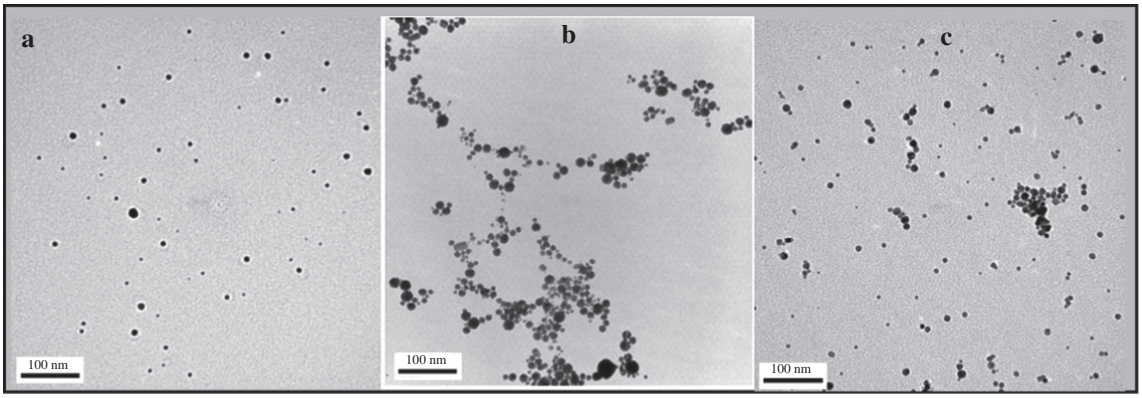

Fig. 4 TEM images of (a) Ag NPs, (b) Ag NPs in the presence of parathion and (c) Ag NPs in the presence of paraoxon-ethyl. The scale bar represents 100 nm.

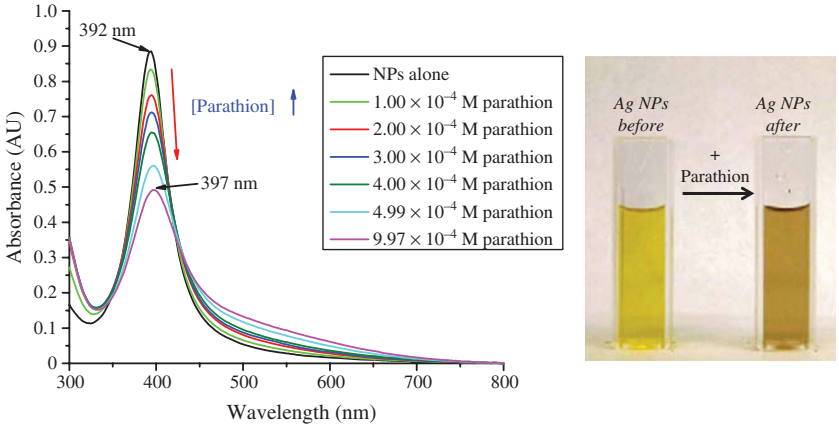

Fig. 5 Changes in the colloid SPR and color of Ag NPs upon the interaction with parathion in the presence of 6.3 mg C/l humic acid at pH 6.

paraoxon-ethyl present in the colloid, the Ag NPs' SPR band absorbed at 394 nm with a slight reduction in absorbance intensity as shown in Fig. 6. Visually, the colloidal Ag NP solution color remained yellow.

The results indicate that the interaction of pesticides that are prevalent in the environment can significantly alter the morphology of nanoparticles. In our case, the nanoparticles were well dispersed in solution but upon interaction with parathion underwent agglomeration. In the presence of humic acid, we do not observe significant agglomeration mainly because the humic acid protects the Ag NP surface preventing its interaction with parathion. Paraoxon on the other hand did not cause agglomeration of the Ag NPs. We believe that this observation is because parathion contains a sulfur group that has a high binding affinity to Ag NPs while the paraoxon has an oxygen group, which has less affinity to the nanoparticle surface. Thus, it is expected that various molecules that exist in the environment will transform the morphology of nanoparticles but that modification will be a result of various components present in the environment. Thus, care must be taken when assessing the effects of various parameters in the environment on ENPs and a clear characterization of all components must be taken into consideration.

Interaction of ENPs with micoorganisms

The study of the interaction of specific materials or chemicals with microorganisms can provide insights into their potential toxicity toward living cells. Such data is useful in evaluating the effects of ENPs especially

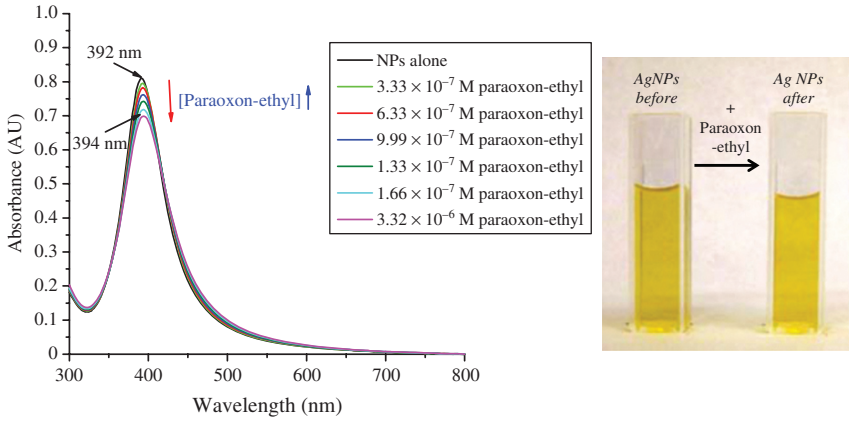

Fig. 6 Changes in the colloid SPR and color of Ag NPs upon the interaction with paraoxon-ethyl in the presence of 6.3 mg C/*l* humic acid at pH 6.

where microorganisms play an important role on the environment. Recently, our group investigated the effect of palladium (Pd) NPs on Gram-positive and Gram-negative bacteria [47]. Our Pd NPs were well-defined and had a narrow size distribution. We found that minute changes in the average diameter of the Pd NPs significantly affected their toxicity toward the bacterial strains such that smaller sizes of particles resulted in a higher mortality rate toward Gram-positive bacteria. These results are important because they demonstrate the influence of particle size on their overall toxicity and thus there must be emphasis on the nanoparticle's size, shape and morphology when reporting the effects of the nanoparticles on microbial species.

Several reports show the effects of metal NPs, primarily Ag NPs on different microorganisms [48–54]. The size-dependent toxicity of Ag NPs on *E. Coli* has also been reported by a number of groups [55–70]. The literature contains a large number of articles that demonstrate the antimicrobial effects of Ag NPs toward various bacterial strains. For example, Kim et al. [53] studied the antimicrobial activity of well-characterized ≈13 nm Ag NPs against yeast, *Escherichia coli* and *Staphylococcus aureus*. Particle shape and size distribution of synthesized Ag NPs were investigated by TEM and a particle size analyzer. The antimicrobial properties of different concentrations of Ag NPs (0.2–33 nM) were evaluated by the Muller Hinton agar (MHA) disk diffusion method. Gentamicin (for *E. coli* and *S. aureus*) and itraconazol (for yeast) were used as positive controls. The results indicated that Ag NPs inhibit the growth of *E. coli* and yeast at low concentrations. However, the effect of Ag NPs on inhabitation of *S. aureus* was mild, indicating that the antimicrobial effects of Ag NPs dependent on the bacterial strains. Electron spin resonance (ESR) spectroscopy was used to determine whether the Ag NPs generated free radicals and if these radicals inhibited bacterial growth. The ESR results revealed that the toxicity of Ag NPs against the bacterial strains was due to the generation of free radicals produced under the experimental conditions.

Morones et al. [71] studied the bactericidal activity of different sizes of Ag NPs against four types of Gram-negative bacteria: *Vibrio cholera, Salmonella typhi, E. coli* and *Pseudomonas aeroginosa*. In order to determine the growth inhibition activities of Ag NPs, each bacterial culture was treated with different concentrations of Ag NPs. The results showed that *E. coli* and *S. typhi* were less resistant relative to *V. cholera* and *P. aeruginosa*. Furthermore, there was no growth of any type of bacteria in the presence of Ag NPs with a concentration higher than 75 μg/mL.

A number of analytical techniques were used to study the effect of Ag NPs on the bacterial strains. As shown in Fig. 7, high angle annular dark field (HAADF) scanning transmission electron microscopy (STEM) was used to elucidate the morphology of the bacterial cells after Ag NP treatment. The data showed the distribution and location of the Ag NPs within the bacterial cells. STEM analysis revealed that the Ag NPs penetrated the bacterial cell, however, if the NPs had agglomerated in the carbon matrix, they were found to only attach to the membrane surface with no cell penetration. The results further indicated that 1–10 nm Ag NPs attach to Gram-negative bacterial cell membranes and prevent regular function, such as respiration and permeability as they can penetrate into the cell and interact with phosphorus- and sulfur-containing compounds like DNA. Moreover, the bactericidal properties of Ag NPs are thought to arise due to the release of Ag ions.

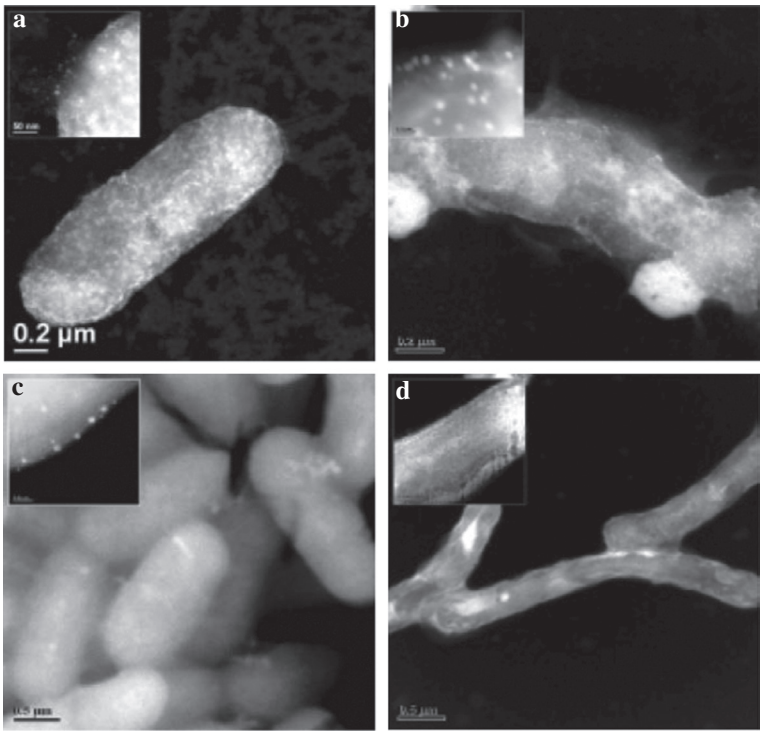

Fig. 7 HAADF STEM image of: (a) *E. coli*, (b) *S. typhi*, (c) *P. aeroginosa* and (d) *V. cholera* that indicates the interaction of the bacteria with the Ag nanoparticles. (Taken with permission from Reference [71].)

Our group has investigated the effect of anchoring a common antibiotic, ampicillin, to Au NPs and Ag NPs surfaces and the effect on bacterial strains. We found that for the bacterial strains, *P. aeruginosa*, *Enterobacter aerogenes*, and *methicillin-resistant Staphylococcus aureus*, that are resistant to ampicillin, overcame ampicillin resistance when ampicillin was functionalized onto the surface of Au NPs and Ag NPs [72]. While Au NPs alone and ampicillin alone were unable to kill any of the bacterial strains tested, the hybrid of ampicillin-Au NPs were found to have a powerful antimicrobial effect of the toxic bacterial strains. In the case of the Ag NPs which have an antimicrobial effect on all the aforementioned bacterial strains, we found that the antimicrobial effect was markedly enhanced upon surface functionalization with ampicillin. While the mechanism of this enhanced antimicrobial effect is still under investigation it is important to note that as the manufacturing and increased use of nanoparticles continues to rise, so will their presence in the environment. Molecules including various contaminants will likely interact with these nanoparticles leading to synergistic effects, some of which are not well studied and the mechanisms are not well understood. Much research is warranted for developing a better understanding of the synergistic effects of functionalized nanoparticles on microbial species, aquatic organisms and the ecosystem.

Shahverdi and coworkers studied the toxic effect of Ag NPs on the activity of different antibiotics including: penicillin G, amoxicillin, carbenicillin, cephalexin, cefixime, erythromycin, gentamicin, amikacin, tetracycline, co-trimoxazole, clindamycin, nitroflurantoin, nalidixin acid and vancomycin against *E. coli* and *S. aureus* bacteria [73]. Ag NPs with a diameter of 25 nm were synthesized using a bioreduction method and were characterized by TEM, energy dispersive spectroscopy (EDS) and UV-visible (UV-vis) absorbance spectroscopy. Disk diffusion assays were applied to evaluate the synergistic effects of Ag NPs toward the growth inhibition properties of antibiotics. The results indicate that the growth inhibition activity of penicillin G, erythromycin, clindamycin, vancomycin and amoxicillin increased in the presence of Ag NPs against *E. coli* and *S. aureus*. However, there was no observed enhanced growth inhibition activity for the other tested antibiotics against both bacterial strains. The highest enhancing effects were observed for vancomycin, amoxicillin and penicillin G against *S. aureus*.

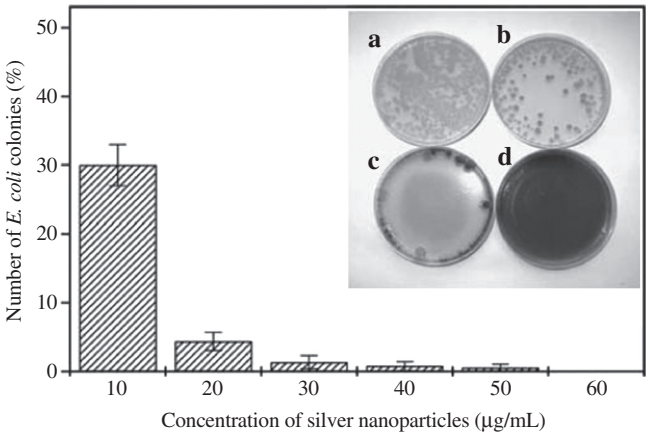

Fig. 8 Number of colonies grown as a function of Ag nanoparticles concentration. (a) 0, (b) 10, (c) 20, and (d) 50 μg cm^{-3}. (Taken with permission from Reference [63].)

In 2004 Sondi et al. reported their study describing the interaction of Ag NPs with *E. coli*, which was used as a model for Gram-negative bacteria [63]. The optical properties of Ag NPs and optical density of the bacteria were evaluated using UV-visible absorbance spectroscopy. The size and morphology of Ag NPs were determined by TEM. However, the bacteria's morphology was investigated using scanning electron microscopy (SEM), X-ray microanalysis and digital imaging systems. In addition, EDS was also applied to determine the chemical composition of the bacterial cell membrane.

The results indicated that Ag NPs showed growth inhibition activity on *E. coli* bacteria. As shown in Fig. 8 the toxicity of Ag NPs on *E. coli* was dose-dependent. Increasing the concentration of Ag NPs caused a decrease in the number of bacterial colonies grown on LB plates.

The EDS analysis of the investigated samples showed that Ag NPs penetrated the cell membrane of the treated bacteria. Images taken by SEM confirmed that the treated bacterial cell walls were significantly damaged as shown in Fig. 9. The TEM images further supported the SEM data and showed that some of the Ag NPs were attached to the surface of bacterial cell membrane while others were able to penetrate the cells.

Pal and coworkers studied the shape-dependent toxicity of Ag NPs against *E. coli* in solution and on agar plates [74]. The synthesized Ag NPs were characterized by UV-visible absorbance spectroscopy and TEM. Morphological changes in the bacterial cell membrane treated with NPs were evaluated by energy-filtering TEM

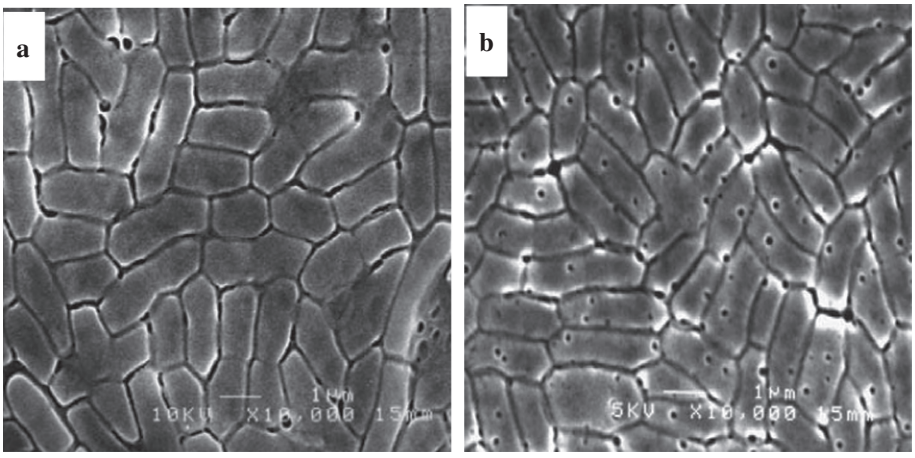

Fig. 9 SEM micrograph of (a) *E. coli* cell and (b) treated *E. coli* cells with 50 μg cm^{-3} Ag NPs. (Taken with permission from Reference [63].)

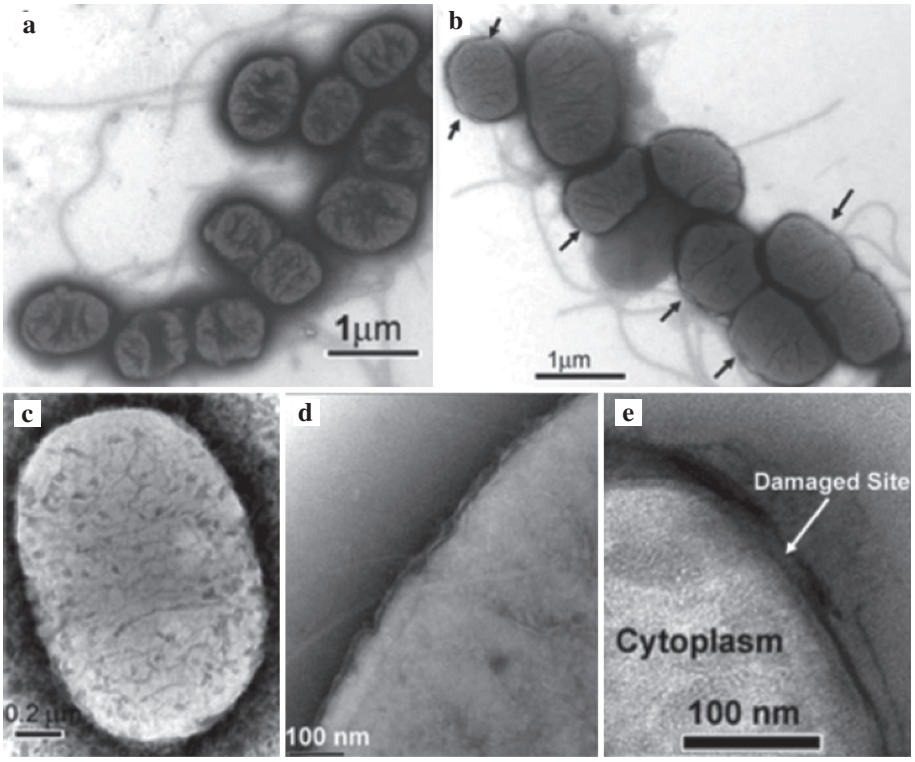

Fig. 10 EFTEM images of *E. coli* cells (a) Untreated cells, (b) Ag ion treated bacteria, arrows show membrane damages, (c) triangular Ag nanoplates treated bacteria, dark pits on the cell surface represent nanoparticles, (d) spherical Ag NPs treated cell, and (e) enlarged image of triangular Ag NPs bacterial cell membrane. (Taken with permission from Reference [74].)

(EFTEM). Kill rates of Ag NPs were evaluated by measuring the optical density at 600 nm of bacterial samples at known concentrations of Ag NPs and the bacterial colony forming units (CFUs). The results indicated that truncated triangular Ag plates with a basal{111} lattice plane showed the highest toxicity on *E. coli* relative to rod-shaped and spherical NPs. The results suggested that the presence of the {111} plane along with the particle nanoscale size were responsible for the toxic effects observed. Figure 10 displays EFTEM images of bacteria treated with different shapes of Ag NPs.

Kumar et al. studied the growth inhibition action of rod shaped Ni NPs against different bacterial strains including: *E. coli*, *S. aureus, P. aeroginosa, Lactobacillus* and *Bacillus subtilis*. In this work Ni NPs with an average diameter of 20–25 nm were synthesized using the reverse micelle method [75]. Nanoparticles were subjected to detailed characterization methods using TEM, X-ray diffraction and Fourier transform infrared (FTIR) spectroscopy. The toxicity of different concentrations of Ni NPs was compared with common antibiotics including ampicillin, penicillin G, gentamicin, clotrimazole, fluconazole, tetracycline and streptomycin. The toxicity of the Ni NPs were evaluated using the agar well diffusion assay method while antibiotics were used as positive controls to compare the growth inhibition activities to Ni NPs. It was found that the bacteria CFU decreased with increasing Ni NP concentration, thus indicating that the Ni NP toxicity was dose-dependent. The location and distribution of the Ni NPs as well as the morphology change of the bacterial cells after exposure to the Ni NPs were examined by TEM. The micrograph results indicated strong damage generated in the cell membranes of treated bacteria.

Similarly, Shamaila and coworkers reported the toxic effects of Ni NPs on *E. coli* cells. Nickel NPs were synthesized by continuous wave (CW) laser ablation of a Ni target in de-ionized water [76]. Dynamic light scattering (DLS), XRD, atomic force microscopy (AFM) and UV-visible absorbance spectroscopy were used to characterize the Ni NPs. Dose-dependent toxicity of Ni NPs on *E. coli* was studied using the serial dilution method and bacterial colonies were measured. The results showed high toxicity of Ni NPs against *E. coli* and determined the highest toxic action of Ni NPs belonged to the most concentrated sample tested.

It is clear that nanoscale materials have strong toxicity toward microorganisms. There are advantages and limitations to this toxicity. The main limitation is that several microorganisms that are present in the environment play a significant role in the fertility of soil and bioremediation. The presence of ENPs in the environment will negatively impact the amount of microorganisms available to aid in environmental processes. Thus, it is essential to control the disposal of ENPs to avoid water and soil pollution. On the other hand, several bacterial strains have developed resistance to antibiotics that were designed to destroy them. The emergence of ENPs that have antimicrobial properties could lead to the development of new materials that are useful for use in areas where a microbe-free environment is needed.

Conclusions and future perspectives

The past decade has seen an increase in the amount of ENPs developed and used in various applications. Commercial products containing ENPs consisting of Ag, and metal oxides for example titanium dioxide and zinc oxide are prevalent. As discussed in this article the antimicrobial effects of Ag NPs is remarkable but the toxicity of Ag NPs is also high. Thus, it is important to evaluate all nanoparticle toxicity and develop guidelines for their handling and proper disposal. The health and safety of ENPs is an important and ongoing area of investigation. Much of the ENP toxicological studies focus on the use of commercially available ENPs. While it is important to perform studies on ENPs that are already in the market, concerns arise that such ENPs lack homogeneity, and thus the toxicity data is not always reproducible. Research is needed that addresses the toxicity of a wide range of ENPs taking into consideration the effects of size, shape and morphology. Analytical techniques that enable *in situ* characterization of ENPs will provide insights into the mechanism of transformation. A majority of the literature focuses on the use of Au and Ag ENPs and it is important to examine other metals particularly those that are being manufactured for catalysis and are in use by industry. It is also important to develop a clear understanding the transformation of ENPs once they enter the environment and the type of interactions they undergo based on the presence of various environmental components.

Acknowledgments: We thank the National Science Foundation Division of Materials Research for support of this work under Award DMR 0963678.

References

[1] G. Ertl, H. Knözinger, F. Schüth, J. Weitkamp (Eds.). *Handbook of Heterogeneous Catalysis*, 2nd ed., Wiley-VCH, Weinheim (2008).
[2] G. A. Somorjai. *Chem. Rev*. **196**, 1223 (1996).
[3] L. N. Lewis. *Chem. Rev*. **93**, 2693 (1993).
[4] T. A. Taton, C. A. Mirkin, R. L. Letsinger. *Science* **289**, 1757 (2000).
[5] G. Tkachenko, H. Xie, D. Coleman, W. Glomm, J. Ryan, M. F. Anderson, S. Franzen, D. L. Feldheim. *J. Am. Chem. Soc*. **125**, 4700 (2003).
[6] H. Wang, D. W. Brandl, P. Nordlander, N. J. Halas. *Acc. Chem. Res*. **40**, 53 (2007).
[7] S. A. Maier, M. L. Brongersma, P. G. Kik, S. Meltzer, A. A. G. Requicha, H. A. Atwater. *Adv. Mater*. **13**, 1501 (2001).
[8] W. Sanders, D. A. Routenberg, B. J. Wiley, Y. Xia, E. R. Dufresne, M. Reed. *Nano Lett*. **6**, 1822 (2006).
[9] S. Jeong, V. Woo, D. Kim, S. Lim, J. S. Kim, H. Shin, Y. Xia, J. Moon. *Adv. Funct. Mater*. **18**, 679 (2008).
[10] J. L. West, N. J. Halas. *Annu. Rev. Biomed. Eng*. **5**, 285 (2003).
[11] P. K. Jain, I. H. El-Sayed, M.A. El-Sayed. *Nano Today* **2**, 18 (2007).
[12] B. Karn, T. Kuiken, M. Otto. *Environ. Health Persp*. **117**, 1823 (2009).
[13] Y. Y. Liu, G. X. Su, B. Zhang, G. B. Jiang, B. Yan. *Analyst* **136**, 872 (2011).
[14] J. H. Han, E. J. Lee, J. H. Lee, K. P. So, Y. H. Lee, G. N. Bae, S. B. Lee, J. H. Ji, M. H. Cho, I. J. Yu. *Inhalation Toxicol.* **20**, 741 (2008).
[15] Y. Fujitani, T. Kobayashi, K. Arashidani, N. Kunugita, K. Suemura. *J. Occup. Environ. Hyg*. **5**, 380 (2008).
[16] B. Yeganeh, C. M. Kull, M. S. Hull, L. C. Marr. *Environ. Sci. Technol*. **42**, 4600 (2008).
[17] E. Demou, W. J. Stark, S. Hellweg. *Ann. Occup. Hyg*. **53**, 829 (2009).
[18] B. Nowack, T. D. Bucheli. *Environ. Pollut*. **150**, 5 (2007).
[19] F. Gottschalk, B. Nowack. *J. Environ. Monit*. **13**, 1145 (2011).

[20] T. M. Scown, R. van Aerle, C. R. Tyler. *Crit. Rev. Toxic*. **40**, 653 (2010).
[21] A. M. Schrand, M. F. Rahman, S. M. Hussain, J. J. Schlager, D. A. Smith, A. F. Syed. *WIREs Nanomed. Nanobiotechnol*. **2**, 544 (2010).
[22] J. Lee, S. Mahendra, P. J. J. Alvarez. *ACS Nano* **4**, 3580 (2010).
[23] D. Maynard, R. J. Aitken, T. Butz, V. Colvin, K. Donaldson, G. Oberdörster, J. R. Philbert, A. Seaton, V. Stone, S. S. Tinkle, L. Tran, N. J. Walker, D. B. Warheit. *Nature* **444**, 267 (2006).
[24] V. L. Colvin. *Nat. Biotech*. **21**, 1166 (2003).
[25] O. S. Ivanova, F. P. Zamborini. *J. Am. Chem. Soc*. **132**, 70 (2010).
[26] T. S. Ahmadi, S. L. Logunov, M. A. El-Sayed. In *Nanostructured Materials: Clusters, Composites, and Thin Films*, V. M. Shalaev and M. Moskovits (Eds.), pp. 125–140, ACS Symposium Series 679; American Chemical Society, Washington, DC (1997).
[27] Y. Li, S.-J. Kim. *J. Phys. Chem, B*. **109**, 12309 (2005).
[28] S. Garbarino, A. Pereira, C. Hamel, E. Irissou, M. Chaker, D. Guay. *J. Phys. Chem. C*. **114**, 2980 (2010).
[29] M. J. Bowers, J. R. McBride, S. J. Rosenthal. *J. Am. Chem. Soc*. **127**, 15378 (2005).
[30] R. S. Varma. *Pure Appl. Chem*. **85**, 1703 (2013).
[31] M. Ganesan, R. Freemantle, S. O. Obare. *Chem. Mater*. **19**, 3464 (2007).
[32] K. J. Major, C. De, S. O. Obare. *Plasmonics* **4**, 61, (2009).
[33] R. G. Freemantle, W. Guo, M. Liu, S.O. Obare. *ECS Transactions* **6**, 93 (2007).
[34] R. Lin, R. G. Freemantle, N. M. Kelly, S.O. Obare, R. Y. Ofoli. *Nanotechnology* **21**, 325605 (2010).
[35] J. F. Liu, Z. S. Zhao, G. B. Jiang. *Environ. Sci. Technol*. **42**, 6949 (2008).
[36] J. Farbrega, S. R. Fawcett, J. C. Renshaw, J. R. Lead. *Environ. Sci. Technol*. **43**, 7285 (2009).
[37] E. Bae, H. J. Park, J. Yoon, Y. Kim, K. Choi, J. Yi. *Korean J. Chem. Eng*. **28**, 267 (2011).
[38] J. Gao, K. Powers, Y. Wang, H. Zhou, S. M. Roberts, B. M. Moudgil, B. Koopman, D. S. Barber. *Chemosphere* **89**, 96 (2012).
[39] R. D. Handy, F. von der Kammer, J. R. Lead, M. Hassellov, R. Owen, M. Crane. *Ecotoxicology* **17**, 287 (2008).
[40] R. Petosa, D. P. Jaisi, I. R. Quevedo, M. Elimelech, N. Tufenkji. *Environ. Sci. Technol*. **44**, 6532 (2010).
[41] B. J. Walker. *Organophosphorus Chemistry*. (Penguin library of physical sciences: Chemistry), Penguin, Middlesex, England, 1972.
[42] R. Reigart, J. Roberts (Eds). *Recognition and Management of Pesticide Poisonings*, 5th ed., Chapter 4. EPA's Office of Pesticide Programs, Arlington, VA (1999).
[43] J. M. Katz, C. K. Winter. *Food Chem. Toxicol*. **47**, 335 (2009).
[44] J. H. Salas, M. M. Gonzalez, M. Noa, N. A. Perez, G. Diaz, R. Gutierrez, H. Zazueta, I. Osuna. *J. Agric. Food Chem*. **51**, 4468 (2003).
[45] R. J. Gillion. *Envrion. Sci. Technol*. **41**, 3408 (2007).
[46] J. E. House, K. A. House. *Descriptive Inorganic Chemistry*, pp. 123–127, Harcourt/Academic Press, San Diego (2001).
[47] C. P. Adams, K. A. Walker, S. O. Obare, K. M. Docherty. *Plos One* **9**, e85981 (2014).
[48] L. M. Stevenson, H. Dickson, T. Klanjscek1, A. A. Keller, E. McCauley, R. M. Nisbet. *Plos One* **9**, e74456 (2013).
[49] C. Greulich, D. Braun, A. Peetsch, J. Diendorf, B. Siebers, M. Epple, M. Koller. *RSC Advances* **2**, 6981 (2012).
[50] T. Klaus, R. Joerger, E. Olsson, C. Granqvist. *Proc. Nat. Acad. Sci. USA* **96**, 13611 (1999).
[51] S. K. Gogoi, P. Gopinath, A. Paul, A. Ramesh, S. S. Ghosh, A. Chattopadhyay. *Langmuir* **22**, 9322 (2006).
[52] C. N. Lok, C. M. Ho, R. Chen, Q. Y. He, W. Y. Yu, H. Sun, P. K. Tam, J. F. Chiu, C. M. Che. *J. Proteome Res*. **5**, 916 (2006).
[53] J. S. Kim, E. Kuk, K. N. Yu, J. H. Kim, S. J. Park, H. J. Lee, S. H. Kim, Y. K. Park, Y. H. Park, C. Y. Hwang, Y. K. Kim, Y. S. Lee, D. H. Jeong, M. H. Cho. *Nanomedicine* **3**, 95 (2007).
[54] C. M. Goodman, C. D. McCusker, T. Yilmaz, V. M. Rotello. *Bioconjugate Chem*. **15**, 897 (2004).
[55] A. K. Suresh, D. A. Pelletier, W. Wang, J. Moon, B. Gu, N. P. Mortensen, D. P. Allison, D. C. Joy, T. J. Phelps, M. J. Doktycz. *Environ. Sci. Technol*. **44**, 5210 (2010).
[56] H. Zhang, G. Chen. *Environ. Sci. Technol*. **43**, 2905 (2009).
[57] L. Wen-Ru, X. Xiao-Bao, S. Qing-Shan, Z. Hai-Yan, O.-Y. You-Sheng, C. Yi- Ben. *Appl. Micobiol. Biotechnol*. **85**, 1115 (2010).
[58] G. A. Martinez-Castanon, N. Nino-Martinez, F. Martinez-Gutierrez, J. R. Martinez- Mendoza, F. Ruiz, J. Ruiz. *J. Nanopart. Res*. **10**, 1343 (2008).
[59] B. Chudasama, A. K. Vala, N. Andhariya, R. V. Mehta, R. V. Upadhyay. *J. Nanopart. Res*. **12**, 1677 (2010).
[60] O. Choi, K. K. Deng, K. K., N.-J. Kim, L. Ross Jr., R. Y. Surampalli, Z. Hu. *Water Res*. **42**, 3066 (2008).
[61] C. Lok, C. Ho, R. Chen, Q. He, W. Yu, H. Sun, P. K. Tam, J. Chiu, C. Che. *J. Biol. Inorg. Chem*. **12**, 527 (2007).
[62] A. Melaiye, Z. Sun, K. Hindi, A. Milsted, D. Ely, D. H. Reneker, C. A. Tessier, W. J. Youngs. *J. Am. Chem. Soc*. **127**, 2285 (2005).
[63] I. Sondi, B. Salopek-Sondi. *J. Coll. Interf. Sci*. **275**, 177 (2004).
[64] F. Martinez-Gutierrez, P. L. Olive, A. Banuelos, E. Orrantia, N. Nino, E. M. Sanchez, F. Ruiz, H. Bach, Y. Av-Gay. *Nanomed. Nanotechnol. Biol. Med*. **6**, 681 (2010).
[65] V. C. Verma, R. N. Kharwar, A. C. Gange. *Nanomedicine* **5**, 33 (2010).
[66] C. Krishnaraj, E. G. Jagan, S. Rajasekar, P. Selvakumar, P. T. Kalaichelvan, N. Mohan. *Colloids Surf. B* **76**, 50 (2010).
[67] S. Sadhasivam, P. Shanmugam, K. Yun. *Colloids Surf., B* **81**, 325 (2010).
[68] N. Drogat, R. Granet, V. Sol, A. Memmi, N. Saad, C. K. Koerkamp, P. Bressollier, P. Krausz. *J. Nanopart. Res*. **13**, 1557 (2010).
[69] G. K. Vertelov, Y. A. Krutyakov, A. Y. Efremenkova, O. V. Olenin, G. V. Lisichkin. *Nanotechnology* **19**, 355707 (2008).

[70] H. H. Lara, N. V. Ayala-Nunez, L. C. I. Turrent, C. R. Padilla. *World J. Microbiol. Biotechnol.* **26**, 615 (2010).
[71] R. Morones, J. L. Elechiguerra, A. Camacho, K. Holt, J. B. Kouri, J. T. Ramírez, M. J. Yacaman. *Nanotechnology* **16**, 2346 (2005).
[72] N. Brown, K. Smith, T. A. Samuels, J. Lu, S. O. Obare, M. E. Scott. *Appl. Environ. Microbiol.* **78**, 2768 (2012).
[73] R. Shahverdi, A. Fakhimi, H. R. Shahverdi, S. Minaian. *Nanomed. Nanotechnol. Biol. Med.* **3**, 168 (2007).
[74] S. Pal, Y. K. Tak, J. M. Song. *Appl. Environ. Microbiol.* **73**, 1712 (2007).
[75] H. Kumar, R. Rani, R. Salar. *J. Chem. Sci.* **1**, 42 (2011).
[76] S. Shamaila, H. Wali, R. Sharif, J. Nazir, N. Zafar, M. S. Rafique. *Appl. Phys. Lett.* **103**, 153701 (2013).